Azimuthal distinguishability of entangled photons generated in spontaneous parametric down-conversion

Clara I. Osorio[1*], Gabriel Molina-Terriza[1,2], Blanca G. Font[1,3] and Juan P. Torres[1,3]

[1]*ICFO-Institut de Ciencies Fotoniques, Universitat Politecnica de Catalunya, Mediterranean Technology Park, Av. del Canal Olmpic s/n, 08860, Castelldefels, Barcelona, Spain*

[2]*ICREA-Institucio Catalana de Recerca i Estudis Avancats, 08010 Barcelona, Spain*

[3]*Department of Signal Theory and Communications, Universitat Politecnica de Catalunya, Jordi Girona 1-3, 08034 Barcelona Spain*

clara.ines.osorio@icfo.es

Abstract: We experimentally demonstrate that paired photons generated in different sections of a down-conversion cone, when some of the interacting waves show Poynting vector walk-off, carry different spatial correlations, and therefore a different degree of spatial entanglement. This is shown to be in agreement with theoretical results. We also discuss how this *azimuthal distinguishing* information of the down-conversion cone is relevant for the implementation of quantum sources aimed at the generation of entanglement in other degrees of freedom, such as polarization.

OCIS codes: (190.4410) Nonlinear optics, parametric processes; (270.0270) Quantum optics ; (270.1670) Coherent optical effects

References and links

1. G. Molina-Terriza, J. P. Torres and L. Torner, "Twisted photons," Nature Phys. **3**, 305 - 310 (2007).
2. A. Vaziri, J. Pan, T. Jennewein, G. Weihs and A. Zeilinger, "Concentration of Higher Dimensional Entanglement: Qutrits of Photon Orbital Angular Momentum," Phys. Rev. Lett. **91**, 227902 (2003).
3. G. Molina-Terriza, A. Vaziri, R. Ursin, and A. Zeilinger, " Experimental Quantum Coin Tossing," Phys. Rev. Lett. **94**, 040501 (2005).
4. J. T. Barreiro, N. K. Langford, N. A. Peters, and P. G. Kwiat , "Generation of Hyperentangled Photon Pairs," Phys. Rev. Lett. **95**, 260501 (2005).
5. J. P. Torres, A. Alexandrescu and L. Torner, "Quantum spiral bandwidth of entangled two-photon states," Phys. Rev. A **68** 050301(R) (2003).
6. C. K. Law and J. H. Eberly, "Analysis and Interpretation of High Transverse Entanglement in Optical Parametric Down Conversion," Phys. Rev. Lett. **92**, 127903 (2004).
7. H. H. Arnaut and G. A. Barbosa, "Orbital and Intrinsic Angular Momentum of Single Photons and Entangled Pairs of Photons Generated by Parametric Down-Conversion," Phys. Rev. Lett. **85**, 286 (2000).
8. A. Mair, A. Vaziri, G. Weihs and A. Zeilinger, "Entanglement of the orbital angular momentum states of photons," Nature **412**, 313-316 (2001).
9. P. S. K. Lee, M. P. van Exter, and J. P. Woerdman, "How focused pumping affects type-II spontaneous parametric down-conversion," Phys. Rev. A **72**, 033803 (2005).
10. P. G. Kwiat, E. Waks, A. G. White, I. Appelbaum and P. H. Eberhard, "Ultrabright source of polarization-entangled photons," Phys. Rev. A **60**, R773 (1999).

#87653 - $15.00 USD Received 17 Sep 2007; revised 12 Oct 2007; accepted 12 Oct 2007; published 22 Oct 2007

11. J. Altepeter, E. Jeffrey, and P. Kwiat, "Phase-compensated ultra-bright source of entangled photons," Opt. Express, **13**, 8951-8959(2005).
12. J. P. Torres, G. Molina-Terriza and L. Torner, "The spatial shape of entangled photon states generated in noncollinear, walking parametric downconversion," J. Opt. B: Quantum Semiclass. Opt. **7**, 235-239 (2005).
13. A. Migdall, "Polarization directions of noncollinear phase-matched optical parametric downconversion output," J. Opt. Soc. Am. B, **14** 1093-1098 (1997).
14. M. H. Rubin, "Transverse correlation in optical spontaneous parametric down-conversion," Phys. Rev. A **54**, 5349 (1996).
15. G. Molina-Terriza, S. Minardi, Y. Deyanova, C. I. Osorio, M. Hendrych and J. P. Torres, "Control of the shape of the spatial mode function of photons generated in noncollinear spontaneous parametric down-conversion," Phys. Rev. A **72**, 065802 (2005).
16. M. V. Fedorov, M. A. Efremov, P. A. Volkov, E. V. Moreva, S. S. Straupe and S. P. Kulik, "Anisotropically and High Entanglement of Biphoton States Generated in Spontaneous Parametric Down-Conversion," Phys. Rev. Lett. **99**, 063901 (2007).
17. G. Molina-Terriza, J. P. Torres and L. Torner, "Management of the Angular Momentum of Light: Preparation of Photons in Multidimensional Vector States of Angular Momentum," Phys. Rev. Lett. **88**, 013601 (2002).
18. M. P. van Exter, A. Aiello, S. S. R. Oemrawsingh, G. Nienhuis, and J. P. Woerdman, "Effect of spatial filtering on the Schmidt decomposition of entangled photons," Phys. Rev. A **74**, 012309 (2006).

1. Introduction

Paired photons entangled in the spatial degree of freedom are represented by an infinite dimensional Hilbert space. This offers the possibility to implement quantum algorithms that either inherently use dimensions higher than two or exhibit enhanced efficiency in increasingly higher dimensions (see [1] and references inside). These include the demonstration of the violation of bipartite, three dimensional Bell inequalities [2], the implementation of the *quantum coin tossing* protocol with qutrits [3], and the generation of quantum states in ultra-high dimensional spaces [4]. Actually, the amount of spatial bandwidth, and the degree of spatial entanglement, can be tailored [5, 6], being possible to control the effective dimensionality where spatial entanglement resides.

The most widely used source for generating paired photons with entangled spatial properties is spontaneous parametric down-conversion (SPDC) [7, 8]. In this process, photons are known to be emitted in cones whose shape depends of the phase matching conditions inside the nonlinear crystal. All relevant experiments reported to date make use of a small section of the full down-conversion cone. But the spatial properties of different sections of the cone have been unexplored experimentally up to now. This could be done, for example, by relocating the single photon counting modules. Then, one question naturally arises: *Are the entangled spatial properties of the photons modified depending of the location in the down-conversion cone where they are detected?*

The answer to this question is of great relevance for the implementation of many quantum information schemes. When considering entanglement in the spatial degree of freedom, one should determine whether pairs of photons with different azimuthal angle of emission might show different spatial quantum correlations, since all quantum information applications are based on the availability and use of specific quantum states.

Additionally, the spatial properties of entangled two-photon states have to be taken into account even when entanglement takes place in other degrees of freedom, such as polarization. In general, it is required to suppress any spatial "which-path" information that otherwise degrades the degree of entanglement. This is especially true for configurations that make use of a large spatial bandwidth [9] and in certain SPDC configurations where horizontally and vertically polarized photons are generated in different sections of the down-conversion cone [10, 11]. Finally, the generation of heralded single photons with well defined spatial properties, i.e. a gaussian shape for optimum coupling into monomode optical fibers, depends on the angle of emission [12].

#87653 - $15.00 USD Received 17 Sep 2007; revised 12 Oct 2007; accepted 12 Oct 2007; published 22 Oct 2007

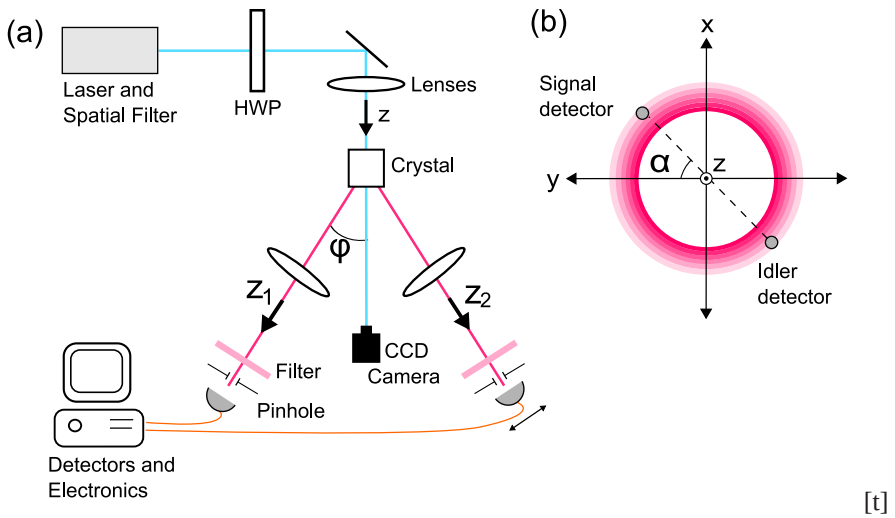

[t]

Fig. 1. (a) Diagram of the experimental set up and (b) The down-conversion cone. Single photon detectors are located in opposite sides of the cone, forming an angle α with the YZ plane.

Here we experimentally demonstrate that the presence of Poynting vector walk-off, which is unavoidable in most SPDC configurations currently being used, introduces *azimuthal distinguishing information in the down-conversion cone*. Paired photons generated with different azimuthal angles show correspondingly different spatial quantum correlations and amount of entanglement. We also show that this spatial distinguishing information can severely degrade the quality of polarization entanglement, since the full quantum state that describes the entangled photons is a nonseparable mixture of polarization and spatial variables.

2. Experimental set-up and results

In Fig. 1 we present a scheme of our experimental set-up. The output beam of a CW diode laser emitting at $\lambda_p = 405nm$, is appropriately spatially filtered to obtain a beam with a gaussian profile, while a half wave plate (HWP) is used to control the polarization. The pump beam is focalized to $w_0 = 136\mu m$ beam waist on the input face of a $L = 5$mm thick lithium iodate crystal, cut at 42° for Type I degenerate collinear phase matching. The generated photons, signal and idler, are ordinary polarized, in opposition to the extraordinary polarized pump beam. The crystal is tilted to generate paired photons which propagate inside the nonlinear crystal with a non-collinear angle of $\varphi = 4^\circ$. Due to the crystal birefringence, the pump beam exhibits Pointing vector walk-off with angle $\rho_0 = 4.9^\circ$, while the generated photons do not exhibit spatial walk-off. Fig. 1(b) represents the transversal section of the down-conversion cone. The directions of propagation of the signal and the idler photons over this ring are determined by the azimuthal angle α, which is the angle between the plane of propagation of the down-converted photons and the YZ plane. To determine experimentally the position of the crystal optics axis, and the origin of α, we measure the relative position of the pump beam in the plane XY at the input and output faces of the nonlinear crystal using a CCD camera.

Right after the crystal, each of the generated photons traverse a $2-f$ system with focal length f=50cm. Low-pass filters are used to remove the remaining pump beam radiation. After the filters, the photons are coupled into multimode fibers. In order to increase our spatial resolution, we use small pinholes of 300μm of diameter. We keep the idler pinhole fixed and measure the

#87653 - $15.00 USD Received 17 Sep 2007; revised 12 Oct 2007; accepted 12 Oct 2007; published 22 Oct 2007

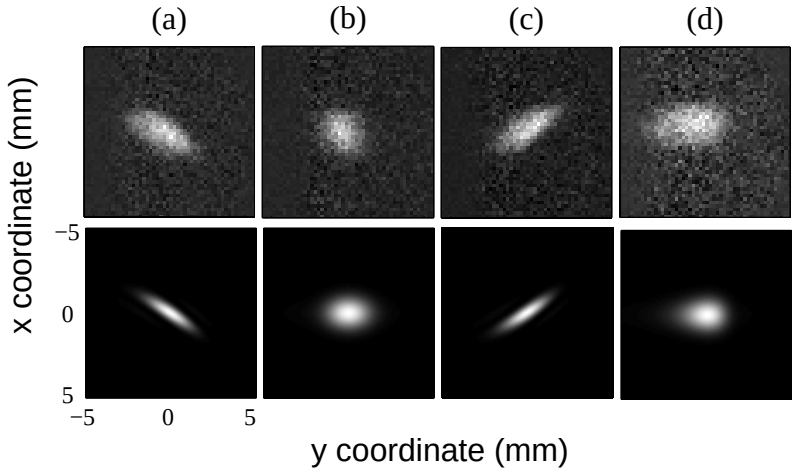

Fig. 2. Images showing the spatial shape of the mode function of the signal photon when measuring coincidences rates. Upper row corresponds to theoretical predictions, and the lower row corresponds to experimental data. (a) $\alpha = 0^\circ$; (b) $\alpha = 90^\circ$; (c) $\alpha = 180^\circ$ and (d) $\alpha = 270^\circ$. See also the corresponding movie.

coincidence rate while scanning the signal photon transverse spatial shape with a motorized XY translation stage. Finally, as we are interested in the different spatial correlations at different azimuthal positions of the downconversion ring, instead of rotating the whole detection system, the nonlinear crystal and the polarization of the pump beam are rotated around the propagation direction. Due to slight misalignments of the rotation axis of the crystal, after every rotation it is necessary to adjust the tilt of the crystal to achieve generation of photons at the same non-collinear angle in all the cases.

Images for different azimuthal sections of the cone were taken. We present a sample of them in the upper row of Fig. 2, which summarizes our main experimental results. Each column shows the coincidence rate for $\alpha = 0^\circ$, 90°, 180° and 270°. The movie shows the experimental and theoretical spatial shape of the signal photon corresponding to other values of the angle α. Each point of these images corresponds to the recording of a 10s measurement. The typical number of coincidences at the maximum is around 10 photons per second. The resolution of the experimental images is 50×50 pixels. The different spatial shapes measured of the mode function of the signal photons clearly show that the down-conversion cone does not posses azimuthal symmetry. This agrees with the theoretical predictions presented in the lower row of Fig. 2. Note that no fitting parameter has been used whatsoever. Slight discrepancies between experimental data and theoretical predictions might be due to the small, but not negligible, bandwidth of the pump beam and to the fact that the resolution of our system is limited by the detection pinholes size.

An interesting feature that can be observed in these images is that the mode function in Fig. 2(b), corresponding to the case $\alpha = 90^\circ$ presents a nearly gaussian shape. We will show below that this effect happens whenever $\varphi \simeq \rho_0$, which corresponds to our experimental conditions. On the other hand the mode function shown in Figs. 2 (a) and (c) are highly elliptical.

3. Azimuthal distinguishability of paired photons generated in different sections of the the down-conversion cone

To gain further insight, we turn to the theoretical description of this problem. The signal photon propagates along the direction $\mathbf{z}_1$ (see Fig. 1) with longitudinal wavevector $k_s = [(\omega_s n_s/c)^2 - |\mathbf{p}|^2]^{1/2}$, and transverse wavevector $\mathbf{p} = (p_x, p_y)$. Similarly, the idler photon propagates along the $\mathbf{z}_2$ direction with longitudinal wavevector k_i, and transverse wavevector $\mathbf{q}$. Here we consider

#87653 - $15.00 USD Received 17 Sep 2007; revised 12 Oct 2007; accepted 12 Oct 2007; published 22 Oct 2007

the signal and idler photons as purely monochromatic, due to the use of a narrow pinhole in the idler side, which selects a very small bandwidth of frequencies of the down-converted ring. Although photons detected in different parts of the down-conversion cone might present slightly different polarizations [13], this is a small effect, and therefore we neglect it.

The quantum two-photon state at the output face of the nonlinear crystal, within the first order perturbation theory, can be written as $|\Psi\rangle = \int d\mathbf{p}d\mathbf{q}\Phi(\mathbf{p},\mathbf{q})a_s^\dagger(\mathbf{p})a_i^\dagger(\mathbf{q})|0,0\rangle$, where the mode function writes [14, 12]

$$\begin{aligned}\Phi(\mathbf{p},\mathbf{q}) = \mathscr{N}\exp\left\{-\frac{(\Gamma L)^2}{4}\Delta_k^2 + i\frac{\Delta_k L}{2}\right\}\\ \times\exp\left\{-\frac{(p_x+q_x)^2 w_0^2 + (p_y+q_y)^2 w_0^2\cos^2\varphi}{4}\right\}\\ \times\exp\left\{-\frac{|\mathbf{p}|^2 w_s^2}{4} - \frac{|\mathbf{q}|^2 w_s^2}{4}\right\}\end{aligned} \tag{1}$$

where $\Delta_k = \tan\rho_0\left[(p_x+q_x)\cos\alpha + (p_y+q_y)\cos\varphi\sin\alpha\right] - (p_y-q_y)\sin\varphi$ comes from the phase matching condition in the z direction, $\mathscr{N}$ is a normalization constant, and we assume that the pump beam shows a gaussian beam profile with beam width w_0 at the input face of the nonlinear crystal. We neglect the transverse momentum dependence of all longitudinal wavevectors. The phase matching function, $sinc(\Delta_k L/2)$ has been approximated by an exponential function that has the same width at the $1/e^2$ of the intensity: $sinc(bx) \simeq \exp[-(\Gamma b)^2 x^2]$, with $\Gamma = 0.455$. The value of w_s describes the effect of the unavoidable spatial filtering produced by the specific optical detection system used. In our experimental set-up, the probability to detect a signal photon at $\mathbf{x_1}$ in coincidence with an idler photon at the fixed pinhole position $\mathbf{x_2} = 0$ is given by $R_c(\mathbf{x_1},\mathbf{x_2}=0) = |\Phi(2\pi\mathbf{x_1}/(\lambda_s f),\mathbf{x_2}=0)|^2$.

Equation 1 shows that the spatial mode function shape shows ellipticity. The amount of ellipticity depends on the non-collinear configuration [15], and on the azimuthal angle of emission (α) due to the presence of spatial walk off. *The latter is the cause of the azimuthal symmetry breaking of the down-conversion cone*. Both effects turn out to be important when the length of the crystal L is larger than the non-collinear length $L_{nc} = w_0/\sin\varphi$ and the walk-off length $L_w = w_0/\tan\rho_0$. Our experimental configuration is fully in this regime. We should notice that in a collinear SPDC configuration, Poynting vector walk-off also introduces ellipticity of the mode function [16].

The theory also predicts the orientation of the spatial mode function of the signal photon, as shown in 2. This is given by the slope $\tan\beta$ in the (p_x, p_y) plane of the loci of perfect phase matching transverse momentum, which writes $\tan\beta = (\sin\varphi - \tan\rho_0\cos\varphi\sin\alpha)/(\tan\rho_0\cos\alpha)$. If $\varphi \simeq \rho_0$ and $\alpha = 90^\circ$, the spatial mode function of the signal photons shows a nearly gaussian shape, due to the compensation of the non-collinear and walk-off effects. All these results are in agreement with experimental data in Fig. 2.

This azimuthal variation of the spatial correlations can be made clearer if we express the mode function of the signal photon, $\Phi_s(\mathbf{p}) = \Phi(\mathbf{p},\mathbf{q}=\mathbf{0})$ in terms of orbital angular momentum modes. The mode function can be described by superposition of spiral harmonics [17] $\Phi_s(\rho,\varphi) = (2\pi)^{-1/2}\sum_m a_m(\rho)\exp(im\varphi)$, where $a_m(\rho) = 1/(2\pi)^{1/2}\int d\varphi\Phi_s(\rho,\varphi)\exp(-im\varphi)$, and ρ and φ are cylindrical coordinates in the transverse wave-number space. The weight of the m-harmonic is given by $C_m = \int\rho d\rho|a_m(\rho)|^2$.

The gaussian pump beam corresponds to a mode with $l_p = 0$, while the idler photon is projected into $\mathbf{q} = 0$, which corresponds to projection into a large area gaussian mode ($l_i = 0$). Figures 3(a) and (b) show the weight of the mode $l_s = 0$, and the weight of all other OAM modes, as a function of the angle α for two different pump beam widths. We observe that the

#87653 - $15.00 USD Received 17 Sep 2007; revised 12 Oct 2007; accepted 12 Oct 2007; published 22 Oct 2007

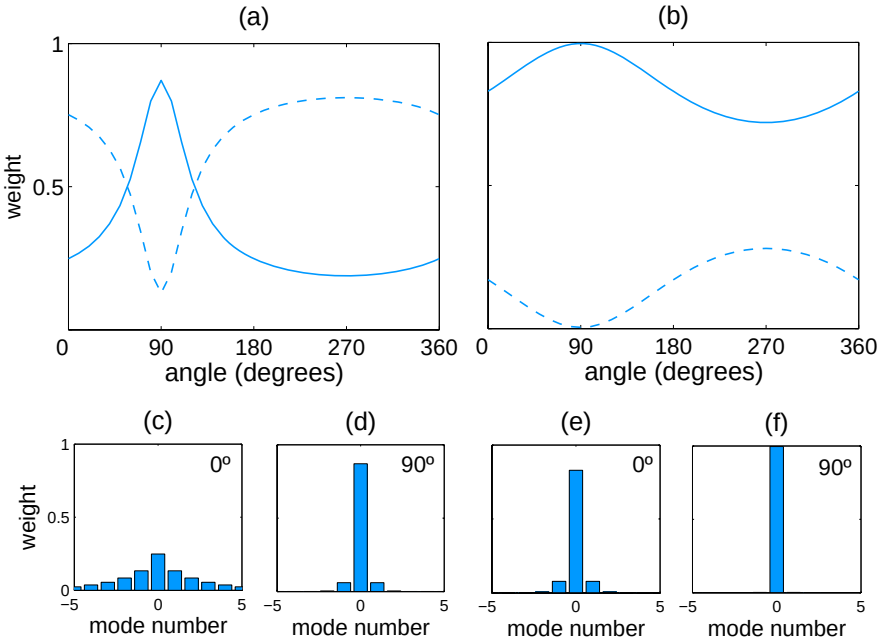

Fig. 3. Weight of the OAM modes $l_s = 0$ (solid line), and all other modes (dashed lines) as a function of the angle α. (a), (c) and (d) $w_0 = 100\mu m$; (b), (e) and (f) $w_0 = 600\mu m$. (c) and (e) show the OAM distribution for $\alpha = 0^\circ$, and (d) and (f) corresponds to $\alpha = 90^\circ$. We assume negligible spatial filtering ($w_s \simeq 0$). Dot-dashed lines: no spatial walk-off.

OAM correlations of the two-photon state change along the down-conversion cone due to the azimuthal symmetry breaking induced by the spatial walk-off. This implies that the correlations between OAM modes do not follow the relationship $l_p = l_s + l_i$. From Fig. 3 it is clearly observed that for larger pump beams the azimuthal changes are smoothed out, since in this case the non-collinear and walk-off lengths are much larger than the crystal length.

Figures 3(c) and 3(d) plots the OAM decomposition for $w_0 = 100\mu$m, and Figs. 3(e) and 3(f) for $w_0 = 600\mu$m, for $\alpha = 0, 90^\circ$. Notice that the weight of the $l_s = 0$ mode is maximum for $\alpha = 90^\circ$, which therefore is the optimum angle for the generation of heralded single photons with a gaussian-like shape. This effect can be clearly observed in Figs. 2(b), 3(d) and 3(f). On the contrary, for $\alpha = 270^\circ$, the combined effects of the noncollinear and walk off effects make the weight of the $l_s = 0$ mode to obtain its minimum value. This is of relevance in any quantum information protocol where the generated photons, no matter the degree of freedom where the quantum information is encoded, are to be coupled into single mode fibers.

Importantly, the degree of spatial entanglement of the two-photon state also shows azimuthal variations, depending on the direction of emission of the down-converted photons. Figure 4 shows the Schmidt number $K = 1/Tr\rho_s^2$, where $\rho_s = Tr_i|\Psi\rangle\langle\Psi|$, is the density matrix that describe the quantum state of the signal photon, after tracing out the spatial variables corresponding to the idler photon. The Schmidt number [6] is a measure of the degree of entanglement of the spatial two photon state, $K = 1$ corresponding to a product state, while larger values of K corresponds to increasingly larger values of the degree of entanglement. The degree of entanglement is maximum for $\alpha = 0$, and minimum for $\alpha = 90^\circ$, as shown in Fig. 4(a). The degree of entanglement is known to decrease with increasing filtering [18], i.e., larger values of w_s, as

#87653 - $15.00 USD Received 17 Sep 2007; revised 12 Oct 2007; accepted 12 Oct 2007; published 22 Oct 2007

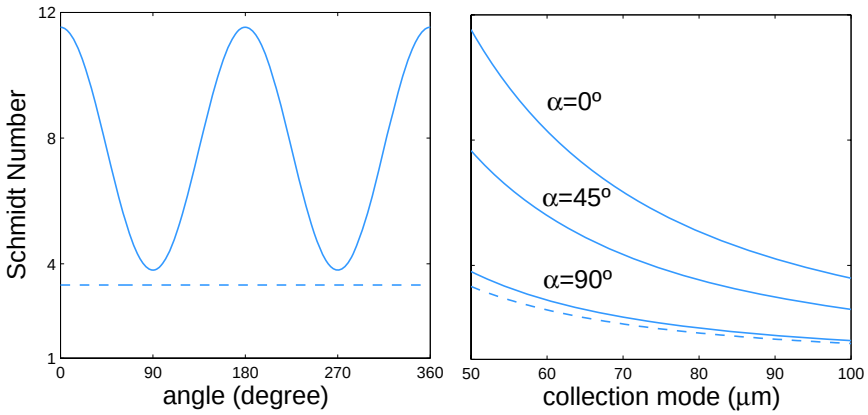

Fig. 4. (a) Schmidt number (K) as a function of the angle α. The width of the collection mode is $w_s = 50\mu$m. (b) Schmidt number as a function of the width of the collection mode for different values of α. In all cases, the pump beam width is $w_0 = 100\mu$m. The Schmidt number for the case with negligible walk-off (dashed lines) is shown for comparison.

shown in Fig. 4(b), and to increase for larger values of the pump beam width (w_0).

4. Effects on the generation of polarization entanglement

The azimuthal distinguishing information introduced by walking SPDC affect the quantum properties of polarization-entangled states, when photons generated in different sections of the down-conversion cone are used. This is the case when using two type I SPDC crystal whose optical axis are rotated 90°. This configuration, originally demonstrated for the generation of polarization-entangled photons [10], has been used as well for the generation of hyperentangled quantum states [4]. The quantum state of the two-photon state writes

$$|\Psi\rangle = \frac{1}{\sqrt{2}} \int d\mathbf{p} d\mathbf{q} \left[\Phi_1(\mathbf{p},\mathbf{q}) |H,\mathbf{p}\rangle_s |H,\mathbf{q}\rangle_i + \Phi_2(\mathbf{p},\mathbf{q}) |V,\mathbf{p}\rangle_s |V,\mathbf{q}\rangle_i\right] \quad (2)$$

$\Phi_1(\mathbf{p},\mathbf{q}) = \Phi(\alpha = 0,\mathbf{p},\mathbf{q}) \exp(ip_y \tan\rho_s L + iq_y \tan\rho_i L)$ describes the spatial shape of the photons generated in the first nonlinear crystal, $\rho_{s,i}$ are the spatial walk-off angles of the down-converted photons traversing the second nonlinear crystal, and $\Phi_2(\mathbf{p},\mathbf{q}) = \Phi(\alpha = 90°,\mathbf{p},\mathbf{q})$ corresponds to the photons generated in the second nonlinear crystal. The quantum state in the polarization space is obtained tracing out the spatial variables, i.e., $\rho_p = Tr_s |\Psi\rangle\langle\Psi|$, which gives

$$\rho_p = \frac{1}{2}\left\{|H\rangle_s |H\rangle_i \langle H|_s \langle H|_i + |V\rangle_s |V\rangle_i \langle V|_s \langle V|_i + \xi \left[|H\rangle_s |H\rangle_i \langle V|_s \langle V|_i + |V\rangle_s |V\rangle_i \langle H|_s \langle H|_i\right]\right\} \quad (3)$$

where $\xi = \int d\mathbf{p} d\mathbf{q} \Phi_1(\mathbf{p},\mathbf{q}) \Phi_2^*(\mathbf{p},\mathbf{q})$.

The degree of mixture of polarization and spatial variables is determined by the purity (P) of the quantum state given by Eq. (3), which writes $P = 1/2\left(1 + |\xi|^2\right)$. The concurrence of the polarization-entangled state, which writes writes $C = |\xi|$, quantifies the quality of the polarization entangled state. Figure 5 shows the concurrence of the quantum state for two different crystal lengths. If spatial walk-off effects are negligible, $|\xi| = 1$ and spatial and polarization

#87653 - $15.00 USD Received 17 Sep 2007; revised 12 Oct 2007; accepted 12 Oct 2007; published 22 Oct 2007

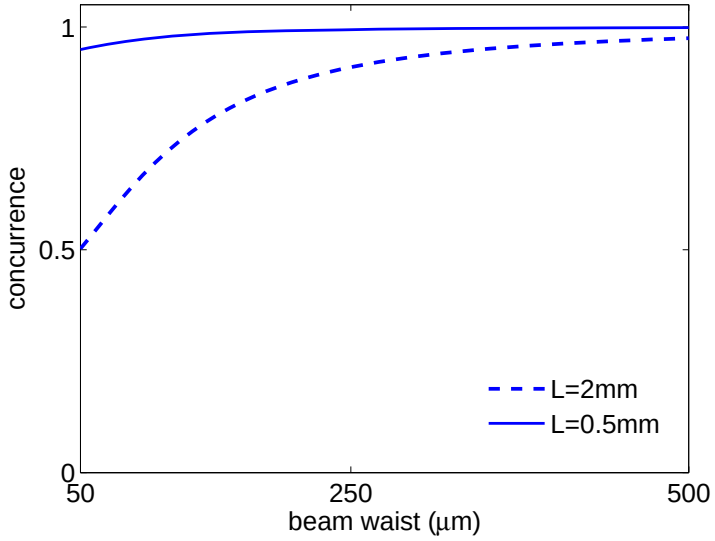

Fig. 5. Concurrence (C) of the polarization entangled bi-photon state generated in a two crystal configuration, as a function of the pump beam, for two different values of the crystal length. The non-collinear angle is $\varphi = 2^{\circ}$, and the pump beam waist is $w_0 = 100\mu$m.

variables can be separated. Therefore, both the purity and the concurrence are equal to 1. This is the case shown in Fig. 5 for a crystal length of $L = 0.5$ mm. Notwithstanding, this is not generally he case, as demonstrated above.

Interestingly, the degree of spatial entanglement of the horizontally polarized photons is unchanged when traversing the second crystal, despite the fact that the down-converted photons shows walk-off. Notwithstanding, the spatial correlations are modified due to the presence of walk-off. It is this effect which enhance spatial distinguishing information and thus degrades the quality of polarization entanglement.

5. Conclusions

We have shown theoretically and experimentally, that the presence of Poynting vector walk-off in SPDC configurations introduces azimuthal distinguishing information of paired photons emitted in different directions of propagation. The quantum correlations of the spatial two-photon state and, consequently, the degree of entanglement show azimuthal variations that are enhanced when using highly focused pump beams and broadband spatial filters. This breaking of the azimuthal symmetry of the down-conversion cone has important consequences when designing and implementing sources of paired photons with entangled properties.

We want to thank X. Vidal and M. Navascues for helpful discussions. This work was supported by projects FIS2004-03556 and Consolider-Ingenio 2010 QOIT from Spain, by the European Commission under the Integrated Project Qubit Applications (Contract No. 015848) and by the Generalitat de Catalunya.

#87653 - $15.00 USD Received 17 Sep 2007; revised 12 Oct 2007; accepted 12 Oct 2007; published 22 Oct 2007